PHYSICAL REVIEW A VOLUME 20, NUMBER 5 NOVEMBER 1979

Fluctuations in superfluorescence

Fritz Haake, Harald King, Guntram Schröder, and Joe Haus
Fachbereich Physik, Gesamthochschule Essen, 43 Essen, Germany

Roy Glauber
Lyman Laboratory of Physics, Harvard University, Cambridge, Massachusetts 02138
(Received 22 March 1979)

We show that certain properties of superfluorescent pulses radiated spontaneously by a system of many initially excited two-level atoms can be described by means of the classical Maxwell-Bloch equations. The quantum fluctuations which initiate the pulse are random initial polarizations. The radiated fields which arise from different initial polarization distributions vary significantly from pulse to pulse. Such variations represent quantum uncertainties amplified to the macroscopic level. Probability distributions are calculated for various parameters characterizing the shape of the output pulse as well as the mean and the variance of the radiated intensity.

I. INTRODUCTION

The problem of superfluorescence is easily stated. A collection of many atoms, raised initially to identical excited states, is allowed to radiate spontaneously and freely. What is sought is a prediction of the properties of the radiated field. The first such prediction, made by Dicke,[1] was that under suitable conditions the atoms will radiate cooperatively. The effect has been observed quite recently in several laboratories.[2]

More detailed theories published in the last several years have clarified the dynamical and statistical properties of superfluorescent systems in qualitative terms.[3] They have done so, however, at the expense of idealizing various aspects of the problem in ways which are to some degree unrealistic. Conflicting views are still heard[4] on which of these simplifications are even permissible in calculating such quantities as the intensity of a superfluorescent pulse.

In one type of idealization, quantum effects are considered to be of minor importance, and the radiation process is treated in the framework of semiclassical theory. The main difficulty then encountered is that the excited state of an atom is, in the absence of an external electromagnetic field, infinitely long-lived. An *ad hoc* way, in which this difficulty has been dealt with, is to endow the atoms with a fictitious initial polarization which then becomes a free parameter. In a second type of idealization the effort has been to retain the most important quantum effects at the expense of reducing drastically the number of degrees of freedom of the fields involved. In several investigations of this kind the atoms have been assumed to interact with only a single mode of the electromagnetic field. Such a single-mode model omits wave-propagation effects and thus cannot be expected to furnish quantitatively correct pulse shapes.

In the present paper we develop an approach which takes careful account of both the quantum-mechanical and wave-propagation aspects of the problem. The quantum-mechanical aspect is treated by a generalization of a mathematical technique which two of us have previously illustrated in connection with the single-mode model.[3(h)] The wave-propagation aspect of the problem is simplified by restricting the excited atoms to a cylindrical volume of Fresnel number unity. We idealize the behavior of this approximately one-dimensional system by allowing wave propagation in one spatial dimension. We then solve the appropriate wave equations.

We show that the dynamics of the radiation process can in effect be regarded as classical at all times if the number of initially inverted atoms, N, is large. The quantum fluctuations, without which the pulse would not be initiated, enter the problem as random initial configurations of the atomic polarization. We calculate the quasiprobability distribution for the initial polarization and find it to be, at each point within the active volume, a Gaussian function with a width of order $1/\sqrt{N}$.

We evaluate the expectation value of the radiated intensity as well as higher-order correlation functions of the radiation field as averages over ensembles of classical solutions obtained by integrating the Maxwell-Bloch equations. These averages take the form of functional integrals in which the Gaussian distribution for the initial polarization appears as a weight. Such expectation values correspond to averages over an ensemble of experimental pulses all originating from identically prepared systems.

Although each experimental pulse corresponds to a classical solution it is impossible to predict

the time dependence of such a pulse since the initial condition for each solution involves, in our formulation, random (i.e., unpredictable) initial values for the atomic polarization. It is another consequence of the random initiation of superfluorescent pulses that their shape varies appreciably from one pulse to another. We calculate the probability distributions for various parameters characterizing the pulse shape. They all have variances comparable in magnitude to their respective mean values. The main results of the present paper are qualitatively similar to those one finds for any process in which fluctuations induce the decay of an unstable equilibrium state of a macroscopic system.[5]

II. QUANTUM-MECHANICAL MAXWELL-BLOCH EQUATIONS

Let us consider N identical two-level atoms distributed uniformly throughout what we shall call the active volume. We can describe the behavior of the atoms by means of the raising operators s_μ^+ with $\mu=1,2,\ldots,N$, the lowering operators s_μ^-, and the inversion operators s_μ^z. These operators obey the angular momentum commutation relations

$$[s_\mu^+, s_\nu^-]=\delta_{\mu\nu}2s_\mu^z, \quad [s_\mu^z, s_\nu^\pm]=\pm\delta_{\mu\nu}s_\mu^\pm. \tag{2.1}$$

Each inversion operator has the eigenvalues $\pm\frac{1}{2}$. Since we will eventually treat the atoms as a continuous medium we find it convenient to combine these operators to form the field densities

$$J_\alpha(\vec{x})=\sum_\mu s_\mu^\alpha \delta^3(\vec{x}-\vec{x}_\mu), \quad \alpha=\pm,z\,. \tag{2.2}$$

For the description of the radiation field and its interaction with the atoms we need the operator for the transverse electric field, which we split into its positive and negative frequency parts,

$$\vec{E}(\vec{x})=\vec{E}^+(\vec{x})+\vec{E}^-(\vec{x})\,. \tag{2.3}$$

These operators have the well-known equal-time commutators

$$[E_i^+(\vec{x}), E_j^-(\vec{x}')]=-2\pi c\hbar\nabla^2\Delta_{ij}^{\mathrm{Tr}}(\vec{x}-\vec{x}')\,. \tag{2.4}$$

Here $\Delta_{ij}^{\mathrm{Tr}}(\vec{x})$ is the convolution of the transverse δ function[6]

$$\delta_{ij}^{3\mathrm{Tr}}(\vec{x})=\delta_{ij}\delta^3(\vec{x})+\frac{1}{4\pi}\frac{\partial^2}{\partial x_i\partial x_j}\frac{1}{|\vec{x}|} \tag{2.5}$$

with the function

$$\Delta(\vec{x})=\int\frac{d^3k}{(2\pi)^3}\frac{e^{i\vec{k}\vec{x}}}{|\vec{k}|}\,. \tag{2.6}$$

The Hamiltonian of the system can be expressed in terms of the fields just introduced. The Hamiltonian of the noninteracting atoms reads

$$H_A=\int d^3x\,\hbar\omega J_z(\vec{x})\,, \tag{2.7}$$

where $\hbar\omega$ is the energy separation of the two levels of an atom. In order to construct the interaction part of the Hamiltonian we note that the operator $i(J_- - J_+)$ may be used to represent the electric polarization density. If we then introduce a vector coupling constant $\vec{g}$, related to the dipole matrix element $e\vec{x}_{12}$ of the atomic transition by $e\vec{x}_{12}=\hbar\vec{g}$, we find that the interaction term can be written

$$H_{AF}=\int d^3x\,\vec{E}(\vec{x})\cdot i\hbar\vec{g}[J_-(\vec{x})-J_+(\vec{x})] \tag{2.8}$$

in the electric dipole approximation. The remaining term in the Hamiltonian is the well-known free-field Hamiltonian.[6]

In order to simplify the problem let us assume the atomic transition to be one that gives rise to light with a single polarization. To be more specific, we take this to be light linearly polarized in the z direction. The treatment of circular polarization would be completely analogous.

The Heisenberg equation of motion for the fields J_α and $\vec{E}$ are easily obtained by using the above commutation relations. The equations for the atomic fields read

$$\begin{aligned}\frac{\partial}{\partial t}J_-(\vec{x},t)&=-i\omega J_-(\vec{x},t)+2\vec{g}\cdot\vec{E}(\vec{x},t)J_z(\vec{x},t)\,,\\ \frac{\partial}{\partial t}J_z(\vec{x},t)&=-\vec{g}\cdot\vec{E}(\vec{x},t)[J_-(\vec{x},t)+J_+(\vec{x},t)]\,.\end{aligned} \tag{2.9}$$

The equation for the electric field is most conveniently written as the inhomogeneous wave equation

$$\left(\nabla^2-\frac{1}{c^2}\frac{\partial^2}{\partial t^2}\right)\vec{E}(\vec{x},t)=-4\pi\nabla^2\vec{P}^{\mathrm{Tr}}(\vec{x},t)\,, \tag{2.10}$$

where

$$P_i^{\mathrm{Tr}}(x,t)=\sum_{j=1,2,3}\int d^3x'\,\delta_{ij}^{3\mathrm{Tr}}(\vec{x}-\vec{x}')i\hbar g_j \times[J_-(\vec{x}',t)-J_+(\vec{x}',t)]$$

is the transverse part of the electric polarization density.

The equations we have constructed to this point represent a general formulation of the microscopic problem of the interaction of the atoms with the radiation field; they bear no reference to the size or shape of the volume containing the atoms. The possibility of choosing the size and shape of that volume freely represents an important means of simplifying the problem. As a first step in this simplification, the choice of a long cylinder lends

a certain one-dimensional character to the problem. We assume that the length l and the diameter d are related by $l \gg d \gg \lambda$. The fields supported by such cylinders differ in character according to whether the Fresnel number $F = d^2/l\lambda$ is greater than or less than unity. In a cylinder with $F > 1$ the axial modes of propagation are quite simple in form since they have little radial dependence. Such a cylinder, however, also supports off-axial modes and would therefore not radiate in a one-dimensional way. The unidirectionality of the radiation may be enhanced by choosing a cylinder with a Fresnel number $F < 1$ since it will then tend to support axial modes only. That can only be done, however, at the expense of introducing a strong radial dependence in the axial modes and significant diffraction losses as well. The latter effects again obstruct a truly one-dimensional description of the radiation process.

Faced with this dilemma, the best that we can do to secure one dimensionality is to compromise by choosing

$$F = d^2/\lambda l \approx 1 . \tag{2.11}$$

Even this choice, which has been made in some of the recent experiments,[2(f)] does not, however, define a strictly one-dimensional problem. In the interest of simplicity what we shall do for the present is to define a one-dimensional problem by treating only axial propagation along the cylinder, and neglecting the radial variation of all the fields. The fields arrived at in this way will presumably not agree precisely with those in the three-dimensional cylinder but should retain much of the same character nonetheless. This is a crucial point to which we shall return in Sec. IX.

A further simplification is possible for systems in which the number density of atoms, n, is large enough so that there are many atoms in every disk-shaped section of the cylinder extending over one wavelength along the axis:

$$nd^2\lambda \gg 1 . \tag{2.12}$$

We may describe such systems in terms of more smoothly varying fields than are defined in Eqs. (2.1)–(2.4). We obtain appropriately smooth fields by averaging the microscopic fields over transverse sections of the cylinder with a volume $\Delta V = d^2 \Delta x$ and a thickness $\Delta x \ll \lambda$:

$$J_\alpha(x,t) = \frac{1}{\Delta V}\int_{\Delta V} d^3x\, J_\alpha(\vec{\mathbf{x}},t) = \frac{1}{\Delta V}\sum_{\vec{\mathbf{x}}_\mu \in \Delta V} s_\mu^\alpha(t) ,$$
$$E(x,t) = \frac{1}{\Delta V}\int_{\Delta V} d^3x\, E_z(\vec{\mathbf{x}},t) . \tag{2.13}$$

These smoothed fields depend on a single discrete spatial coordinate x. We shall find it convenient, however, to adopt the point of view of a macroscopic continuum theory and thus in fact to consider x as a continuous variable.

We can construct the equations of motion for the smoothed fields just defined by carrying out the averaging operation $(1/\Delta V)\int_{\Delta V} d^3x$ in the Heisenberg equations (2.9) and (2.10) and replacing the averages of products of microscopic operators with products of the averages of the individual operators. These equations of motion have the same appearance as the Heisenberg equations (2.9) and (2.10) save for the replacements $\vec{\mathbf{x}} \to x$ and $\nabla^2 \to \partial^2/\partial x^2$.

We can take further advantage of the cylindrical geometry by representing our smoothed fields as monochromatic plane waves $\exp \pm i(kx - \omega t)$ which are subject to slow modulation in space and time. The spatial modulation is assumed slow over distances of order λ and the temporal modulation slow over the oscillation period ω^{-1}. We implement this assumption by introducing dimensionless envelope operators $\hat{E}_R^\pm$, $\hat{E}_L^\pm$, $\hat{R}_\pm$, and $\hat{L}_\pm$ for the various right- and left-going waves and the operator $\hat{Z}$ to represent the inversion as follows:

$$E^\pm(\vec{\mathbf{x}},t) = \frac{1}{2g\tau}\left[e^{\pm i(kx-\omega t)}\hat{E}_R^\pm\left(\frac{x}{l},\frac{t}{\tau}\right) + e^{\mp i(kx+\omega t)}\hat{E}_L^\pm\left(\frac{x}{l},\frac{t}{\tau}\right)\right] ,$$
$$J_\pm(\vec{\mathbf{x}},t) = \frac{n}{2}\left[e^{\mp i(kx-\omega t)}\hat{R}_\pm\left(\frac{x}{l},\frac{t}{\tau}\right) + e^{\pm i(kx+\omega t)}\hat{L}_\pm\left(\frac{x}{l},\frac{t}{\tau}\right)\right] ,$$
$$J_z(\vec{\mathbf{x}},t) = \frac{n}{2}\hat{Z}\left(\frac{x}{l},\frac{t}{\tau}\right) . \tag{2.14}$$

Note that we have introduced several factors into these equations in order to render both the envelope operators and their arguments dimensionless. In particular, distances are measured in terms of the length l and times in terms of a unit τ which we shall presently identify with the superfluorescence time. Furthermore, in these equations g is the component of the coupling constant $\vec{\mathbf{g}}$ parallel to the electric field, i.e., in the z direction. Finally, we have used circumflexes to distinguish the envelope operators defined here from some c-number fields we shall associate with them at a later point.

While the unit of time τ in Eq. (2.14) is arbitrary, a natural choice which has been made in previous work[3(f),4] is the superfluorescence time

$$1/\tau = 2\pi\hbar g^2 nkl = \tfrac{3}{8}\pi\lambda^2 nl/\tau_0 , \tag{2.15}$$

where $1/\tau_0$ is the natural linewidth of the transition. It is the inverse proportionality of τ to the number density n which makes it a unit well suited to the discussion of radiation pulses with peak in-

tensities proportional to n^2. Another property of τ is closely related. Its inverse may be regarded as the natural linewidth $1/\tau_0$ multiplied by the number of atoms $N=nd^2l$ and by a geometrical factor, which for the case of Fresnel number 1, is in the order of magnitude of the ratio of the solid angle of the diffraction cone λ^2/d^2 to the total solid angle 4π. We may also note that the time τ is related to the cooperation length l_c defined by Arecchi and Courtens[7] via

$$l_c^2=lc\tau . \tag{2.16}$$

We now construct the equations of motion for the envelope operators $\hat{R}_\pm$, $\hat{L}_\pm$, $\hat{Z}$, and $\hat{E}^\pm_{R,L}$ by inserting the decompositions (2.14) in the equation of motion for the smoothed fields (2.13), eliminating the various plane-wave phase factors, and at the same time neglecting rapidly oscillating terms. In this way we obtain the Maxwell-Bloch equations in the slowly varying envelope approximation. These equations which are familiar from semiclassical radiation theory take the form

$$\begin{aligned}
&\frac{\partial}{\partial t}\hat{R}_\pm=\hat{Z}\hat{E}^\mp_R ,\\
&\frac{\partial}{\partial t}\hat{L}_\pm=\hat{Z}\hat{E}^\mp_L ,\\
&\frac{\partial}{\partial t}\hat{Z}=-\tfrac{1}{2}(\hat{R}_+\hat{E}^+_R+\hat{L}_+\hat{E}^+_L+\text{H.c.}) ,\\
&\left(\frac{\partial}{\partial x}+\frac{\alpha\partial}{\partial t}\right)\hat{E}^\pm_R=\hat{R}_\mp ,\\
&\left(\frac{-\partial}{\partial x}+\frac{\alpha\partial}{\partial t}\right)\hat{E}^\pm_L=\hat{L}_\mp ,
\end{aligned} \tag{2.17}$$

with

$$\alpha=l/c\tau=(l/l_c)^2 . \tag{2.18}$$

The parameter α will play an important role in our further considerations.

For our discussion of superfluorescence we have to solve the Maxwell-Bloch equations (2.17) with an appropriate initial condition for each envelope operator and with the boundary condition that no external signals impinge on the cylinder at $x=0$ and $x=1$. This is of course a simpler boundary condition than we would have to pose for a second-order wave equation like Eq. (2.10) and it implies that no reflection takes place at either end of the cylinder. That is in fact not an unrealistic simplification since care has usually been taken in superfluorescence experiments to render such reflection effects negligible.

This quantum-mechanical problem would, because of the nonlinearity of the equations of motion, be quite difficult to solve were we not concerned with systems consisting of many atoms. For these, in fact, the dynamics of the radiation process becomes essentially classical, as we shall show below.

III. INITIAL EXPECTATION VALUES

We may gain further insight into the nature of the spontaneous radiation process by considering the expectation values of products of initial polarization operators. The quantum state in which these expectation values must be evaluated is the vacuum state for the electromagnetic field and the excited state for each atom, $|\text{vac},\{\uparrow\}\rangle$.

Intensity measurements on the electromagnetic field characteristically detect expectation values of normally ordered products of electric field operators such as

$$\langle\text{vac},\{\uparrow\}|\hat{E}^-_R(x,t)\hat{E}^+_R(x',t')|\text{vac},\{\uparrow\}\rangle .$$

Since $\hat{R}_+$ is the source of $\hat{E}^-_R$ we need to know the correspondingly ordered expectation values

$$\langle\{\uparrow\}|\hat{R}_+(x,0)\hat{R}_-(x',0)|\{\uparrow\}\rangle .$$

In order to calculate the latter we first use Eqs. (2.13) and (2.14) to express the polarization envelopes and the smoothed inversion density in terms of the atomic operators s^α_μ as

$$\begin{aligned}
&\hat{R}_\pm(x)=e^{\mp i2kl x}\hat{L}_\pm(x)=\frac{2}{n\Delta V}e^{\pm ikl x}\sum_{\vec{x}_\mu\in\Delta V}s^\pm_\mu ,\\
&\hat{Z}(x)=\frac{2}{n\Delta V}\sum_{\vec{x}_\mu\in\Delta V}s^z_\mu .
\end{aligned} \tag{3.1}$$

These equations refer to a discrete sequence of values of the coordinate x.

We immediately obtain from these expressions the single-point expectation values

$$\begin{aligned}
&\langle\{\uparrow\}|\hat{R}_\pm(x,0)|\{\uparrow\}\rangle=\langle\{\uparrow\}|\hat{L}_\pm|\{\uparrow\}\rangle=0 ,\\
&\langle\{\uparrow\}|\hat{Z}(x,0)|\{\uparrow\}\rangle=1 ,
\end{aligned} \tag{3.2}$$

and the two-point function

$$\langle\{\uparrow\}|\hat{R}_+(x,0)\hat{R}_-(x',0)|\{\uparrow\}\rangle=\frac{4}{n\Delta V}\delta_{xx'}=\frac{4}{N}\frac{\delta_{xx'}}{\Delta x} , \tag{3.3}$$

where $\delta_{xx'}$ is the Kronecker symbol. We now revert to the macroscopic continuum description by replacing the expression $\delta_{xx'}/\Delta x$ by the δ function $\delta(x-x')$. In this way we obtain

$$\langle\{\uparrow\}|\hat{R}_+(x,0)\hat{R}_-(x',0)|\{\uparrow\}\rangle=(4/N)\delta(x-x') \tag{3.4}$$

and a similar result for the two-point function $\langle\hat{L}_+\hat{L}_-\rangle$.

Moreover, we find for the multipoint functions $\langle(\hat{R}_+)^j(\hat{R}_-)^j\rangle=\langle(\hat{L}_+)^j(\hat{L}_-)^j\rangle$, as long as the exponent j is small compared to the number of atoms in the

volume $\Delta V = d^2 l \Delta x$:

$$\langle\{\uparrow\}|\hat{R}_+(x_1)\cdots\hat{R}_+(x_j)\hat{R}_-(x_1')\cdots\hat{R}_-(x_j')|\{\uparrow\}\rangle$$
$$=\sum_P \langle\hat{R}_+(x_1)\hat{R}_-(x_1')\rangle\cdots\langle\hat{R}_+(x_j)\hat{R}_-(x_j')\rangle$$
$$=\left(\frac{4}{N}\right)^j\sum_P \delta(x_1-x_1')\cdots\delta(x_j-x_j')\,, \qquad (3.5)$$

where the sums run over all $j!$ permutations of the primed coordinates. In the limit $n\Delta V \gg 1$ these relations hold up to high orders of j. In that case they express a composition law for the correlation functions which is characteristic of classical complex Gaussian stochastic processes.

A complete characterization of the initial state of our system in terms of expectation values must include moments of the form

$$\langle(\hat{E}_R^-)^l(\hat{E}_R^+)^{l'}(\hat{E}_L^-)^m(\hat{E}_L^+)^{m'}$$
$$\times(\hat{R}_+)^p(\hat{L}_+)^q(\hat{Z})^r(\hat{L}_-)^{q'}(\hat{R}_-)^{p'}\rangle\,. \qquad (3.6)$$

Since the initial state is the vacuum state for the electromagnetic field these expectation values all vanish unless $l=l'=m=m'=0$. They also vanish for $p+q\neq p'+q'$ and are, moreover, negligibly small unless $p=p'$ and $q=q'$. In the limit $\Delta V n \gg 1$ and for $p+q \ll \Delta V n$ they do not depend on the exponent r and factorize in terms of the polarization correlation functions to

$$\langle(\hat{R}_+)^p(\hat{R}_-)^p\rangle\langle(\hat{L}_+)^q(\hat{L}_-)^q\rangle\,.$$

We can therefore conclude that the initial fields behave in effect like classical fields. The classical fields corresponding to the initial atomic inversion operator $\hat{Z}$ and to the initial electric field envelopes $E_{R,L}^{\pm}$ have the sharp values $Z=1$ and $E_{R,L}^{\pm}=0$, respectively. The classical fields corresponding to the initial polarizations, however, take on random values with Gaussian statistics. To be more specific, we can calculate initial expectation values of operator products ordered in the sense indicated in Eqs. (3.6) as moments of a quasiprobability distribution. This distribution reads, if the coordinate x is considered as a discrete variable,

$$P[(E_{R,L}^{\pm},R_{\pm},L_{\pm},Z)]$$
$$\sim\prod_x(\delta^2[E_R^+(x)]\delta^2[E_L^+(x)]\delta[Z(x)-1]$$
$$\times\exp\{-(N/4)\Delta x[|R_+(x)|^2+|L_+(x)|^2]\}) \qquad (3.7)$$

IV. CLASSICAL TRAJECTORIES

We shall now show that the statistical behavior of our system can be conveniently represented in terms of classical stochastic fields not only initially but at all later times as well. Let us begin by considering the early stages of the radiation process for which the depletion of the atomic excitation can still be neglected. In that regime the Maxwell-Bloch equations are linear and yield the electric field operators as the following linear functional of the initial field operators[3(v)]:

$$\hat{E}_R^{\mp}(x,t)=\int_0^x dx'\,\hat{R}_{\pm}(x-x',0)\Theta(t-\alpha x')I_0\{2[x'(t-\alpha x')]^{1/2}\}$$
$$+\int_0^x dx'\hat{E}_R^{\mp}(x-x',0)\Theta(t-\alpha x')\alpha\left(\frac{x'}{t-\alpha x'}\right)^{1/2}I_1(2[x'(t-\alpha x')]^{1/2})+\Theta(\alpha x-t)\hat{E}_R^{\mp}(x-t/\alpha,0)\,; \qquad (4.1)$$

a similar expression may be derived for $\hat{E}_L^{\mp}(x,t)$. Here Θ is the unit step function and I_n the modified Bessel function of order n.[8]

The expectation value of the intensity of radiation at the right end of the active volume, $x=1$, can now be written

$$I(t)=\langle\text{vac},\{\uparrow\}|\hat{E}_R^-(1,t)\hat{E}_R^+(1,t)|\text{vac},\{\uparrow\}\rangle$$
$$=\frac{4}{N}\int_0^1 dx\,\Theta(t-\alpha x)\{I_0(2[x(t-\alpha x)]^{1/2})\}^2, \qquad (4.2)$$

where we have used Eq. (3.4). Normally ordered correlation functions involving higher-order products of the electric field operators can be constructed similarly by invoking Eq. (3.5). These higher-order correlation functions also follow the composition law characteristic of complex Gaussian stochastic processes.

The result, (4.1), holds irrespective of whether the fields involved are quantum-mechanical operators of c numbers. The radiated intensity as given by Eq. (4.2), as well as its higher-order generalizations, can thus be obtained by interpreting the linearized Maxwell-Bloch equations as classical equations for c number fields and by replacing the quantum-mechanical initial-state average with an average over initial configurations of these fields according to the weight functional (3.7).

In such an interpretation the quantum fluctuations inherent in the radiation pulse appear as due not to the dynamics of the system but to the fact that the polarization is initially random. This random-

ness expresses an intrinsically quantum-mechanical uncertainty. Since the operators for the inversion and the polarization do not commute, both $\hat{R}_\pm$ and $\hat{L}_\pm$ must have nonvanishing dispersions in the atomic initial state $|\{\uparrow\}\rangle$ which is an eigenstate of $\hat{Z}$.

We should emphasize that it is only in the limit of large N that we can reasonably think of the early stages of the radiation process as having classical deterministic dynamics and Gaussian random initial conditions for the polarization fields. One reason is that the validity of Eq. (3.5) requires N to be very large and another is that the linear regime, $Z(x,t)\approx 1$, cannot hold for any interesting length of time unless N is large.

In the limit of large N the above interpretation remains equally valid in the later nonlinear regime. The initial fields $R_\pm$ and $L_\pm$ are not likely, in typical realizations, to greatly exceed in magnitude a small value of order $1/\sqrt{N}$. However, as soon as the ensuing amplification process has brought about values of the polarization and the electric field which do greatly exceed the magnitude of quantum fluctuations, quantum mechanics can be dispensed with in treating the further time development of the system. That will be so throughout the nonlinear regime. Only at very large times when the atomic system has come close to the ground state and radiates quite weakly can the correspondence principle no longer be invoked in this way.

We may conclude, then, that all normally ordered correlation functions of the electric field can be calculated as if the radiation process were a classical stochastic process with deterministic dynamics but random initial values of the polarizations. To be more specific, we can solve the Maxwell-Bloch equations (2.17) as c number equations. As an initial condition at $t=0$, we require that the electric field be zero everywhere and that the inversion be unity; the polarization envelopes $R_\pm(x,0)$ and $L_\pm(x,0)$, however, are allowed to take on arbitrary complex values. Let us denote the resulting right- and left-going electric fields as

$$E^\pm_{R,L}(x,t,[R_\pm(x,0),L_\pm(x,0)]). \tag{4.3}$$

Of course, E^+ and E^- are now complex conjugates to one another. We will refer to these solutions as the classical trajectories of the electric field. In order to calculate the nth normally ordered intensity moment for the radiated field we average the nth power of the squared modulus of the electric field (4.3) over the initial polarizations with the Gaussian weight given in Eq. (3.7). We then obtain the expression

$$I^n(t)=\int d^2R_+(x)\,d^2L_+(x)\,P([R_+(x),L_+(x)]) \times |E^+_R(x=1,t,[R_+(x),L_+(x)])|^{2n}, \tag{4.4}$$

with

$$P([R_+(x),L_+(x)]) \sim \exp\left(-\frac{N}{4}\int_0^1 dx\,[\,|R_+(x)|^2+|L_+(x)|^2]\right). \tag{4.5}$$

The integrals in Eq. (4.4) extend over the complex plane for both $R_+(x)$ and $L_+(x)$ at each point x. In the limit of continuous x these integrals constitute a functional integral. In Eq. (4.4) we could equally well use the classical trajectory of the left-going electric field $E^+_L(x=0,t)$ since the Maxwell-Bloch equations (2.17) are symmetric under the transformation $R\Leftrightarrow L$, $x\Leftrightarrow 1-x$.

We have established the foregoing strategy for calculating expectation values on the basis of the rigorous treatment of the early-stage linear regime and of the correspondence principle. A detailed derivation of the results we have outlined in the present section is given in the Appendix.

Up to now we have used the classical trajectories as ingredients of a particularly convenient scheme for calculating quantum-mechanical expectation values without discussing their observability. In fact, each of the calculated trajectories corresponds to a possible experimental pulse as soon as the early-stage amplification has brought the field intensities to the macroscopic level. It is then possible to measure all of the fields, $R_\pm$, $L_\pm$, Z, and $E^\pm_{R,L}$, without thereby disturbing their values appreciably.

We should emphasize, however, that the earliest stages of an experimental pulse cannot be regarded as a classical process. In that regime the electric field and the polarization have not yet risen above the level of quantum fluctuations and would therefore be greatly disturbed by measurements. During such early times a single classical trajectory has no physical meaning beyond being an ingredient in calculating expectation values according to Eq. (4.4).

We should also point out that it is impossible to predict the time dependence of any single experimental pulse even though the pulse dynamics is classical for times relevant to macroscopic observations. The reason we cannot is that the initial polarization from which the pulse begins is intrinsically random in character. It is likewise impossible, as a matter of principle, to ascertain *a posteriori* from which initial polarizations $R_\pm(x,0)$ and $L_\pm(x,0)$ a given experimental pulse has originated since during its earliest stages the pulse does

not behave classically.

Yet another aspect of the pulse generation deserves emphasis. In spite of the classical nature each experimental pulse has while its intensity is large we must expect large fluctuations in an ensemble of such pulses. Indeed, since the initial polarizations triggering the radiation process are intrinsically random, i.e., uncorrelated from one pulse to another, the shapes of different pulses will vary considerably. Such variations are macroscopic manifestations of quantum uncertainties.

V. TWO CONSERVATION LAWS

The classical versions of the Maxwell-Bloch equations (2.17) contain two conservation laws which are both useful in the later analysis. The first of these laws implies that the quantity

$$Z(x,t)^2 + |R_+(x,t)|^2 + |L_+(x,t)|^2$$

is time independent. We can check the conservation of this quantity by considering its time derivative and using the first three of Eqs. (2.17). Since according to Eq. (3.7) the initial inversion is unity while the initial polarizations are unlikely to assume values greatly exceeding the magnitude $1/\sqrt{N}$ we can write the conservation law as

$$Z(x,t)^2 + |R_+(x,t)|^2 + |L_+(x,t)|^2 = 1 . \tag{5.1}$$

We should point out that this classical law has its quantum-mechanical origin in the fact that each two-level atom is equivalent to a spin-$\frac{1}{2}$ system and that the squared length of the corresponding spin vector, $\vec{s}_\mu^{\,2} = (s_\mu^z)^2 + s_\mu^+ s_\mu^- - 2s_\mu^z$, is conserved by the Hamiltonian defined in Eqs. (2.7) and (2.8).

The second conservation law we shall need is global in character and implies that the number of light quanta with energies near $\hbar\omega$ plus the number of excited atoms is a constant of the motion. The constancy of this quantity is due to our neglect of rapidly oscillating terms in the Maxwell-Bloch equations (2.17). We can derive the law from Eqs. (2.17) by multiplying the differential equation for E_R^+ by E_R^- and that for E_L^+ by E_L^- and considering the sum of the resulting equations. We thus obtain

$$\left(\frac{\partial}{\partial x} + \alpha\frac{\partial}{\partial t}\right)\left|E_R^+\right|^2 + \left(\frac{-\partial}{\partial x} + \alpha\frac{\partial}{\partial t}\right)\left|E_L^+\right|^2 = R_+E_R^+ + L_+E_L^+ + \text{c.c.} = -2\dot{Z} .$$

We now integrate over the time from 0 to t and over the spatial coordinate from 0 to 1 and find, by invoking our initial and boundary conditions, the conservation law

$$\frac{1}{2}\int_0^t dt'\left[|E_R^-(1,t')|^2 + |E_L^-(0,t')|^2\right] + \frac{\alpha}{2}\int_0^1 dx\left[|E_R^-(x,t)|^2 + |E_L^-(x,t)|^2\right] + \int_0^1 dx\, Z(x,t) = 1 . \tag{5.2}$$

VI. DOMINANCE OF LONG-WAVELENGTH FLUCTUATIONS

There is still more insight to be gained into the dynamics of the radiation process from the analysis of its early-state linear behavior. Let us decompose the electric field envelope into plane waves according to the double Fourier integral

$$E_R^+(x,t) = \int_{-\infty}^{+\infty}\frac{d\omega}{2\pi}\int_{-\infty}^{+\infty}\frac{dk}{2\pi}E_R^+(k,\omega)e^{i(kx-\omega t)} \tag{6.1}$$

and represent the polarization field $R_-(x,t)$ by a temporal Fourier integral as

$$R_-(x,t) = \int_{-\infty}^{+\infty}\frac{d\omega}{2\pi}e^{-i\omega t}R_-(x,\omega) . \tag{6.2}$$

By Fourier analyzing the linearized versions of the Maxwell-Bloch equations (2.17) in terms of the representations (6.1) and (6.2) and eliminating the amplitude $R_-(x,\omega)$ we find a homogeneous linear algebraic equation for the amplitude $E^+(k,\omega)$ and the following dispersion relation $\omega = \omega(k)$ for the frequency of the plane electromagnetic waves,

$$\omega^2 - \omega k/\alpha + 1/\alpha = 0 . \tag{6.3}$$

The solution $\omega(k)$ of this equation is depicted in Fig. 1. We may note the appearance of asymptotes corresponding to the frequencies of free photons and of free two-level atoms. The most noteworthy feature of the dispersion curve is, however, the gap of wave numbers,

$$|k| < 2\sqrt{\alpha} = 2l/l_c , \tag{6.4}$$

within which there are no real frequencies avail-

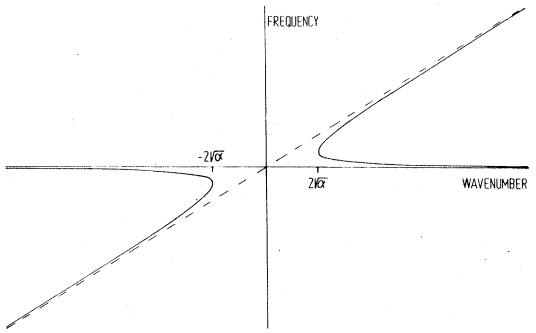

FIG. 1. Dispersion relation (6.3).

able for real values of k. Waves with wave numbers in this "amplification gap" will have complex solutions for ω, one of which will correspond to an exponential increase with time. Such waves will therefore be rapidly amplified and tend to dominate the electric field.

Since the polarization field $R_-(x,t)$ vanishes outside the active volume it is advantageous to represent it by the spatial Fourier series

$$R_-(x,t)=\sum_{\nu=0,\pm1,\ldots} r_\nu(t)e^{i2\pi\nu x} \tag{6.5}$$

rather than by an integral. We then find from the linearized version of motion for R_- in (2.17) the following linear relation between the amplitudes of the discrete polarization modes and the continuous electric field modes,

$$E_R^+(k,\omega)=-i\omega\sum_\nu r_\nu(\omega)c_\nu(k)\,, \tag{6.6}$$

where $r_\nu(\omega)$ is the temporal Fourier transform of the coefficient $r_\nu(t)$ and $c_\nu(k)$ is a coupling constant given by

$$c_\nu(k)=-i\frac{e^{i(2\pi\nu-k)}-1}{2\pi\nu-k}. \tag{6.7}$$

We see that the coupling is strong only for wave numbers

$$k\approx k_\nu\equiv 2\pi\nu,\quad \nu=0,\pm1,\pm2,\ldots \tag{6.8}$$

We may conclude that only polarization modes with k_ν within the amplification gap will be dynamically important. The simplest type of problem to treat is therefore characterized by

$$\alpha=l/l_c<1\,, \tag{6.9}$$

since then only the polarization mode with $\nu=0$ lies within the amplification gap.

The result just obtained is of crucial importance to our further investigations. It means that for $\alpha<1$ the contributions to the electric field of the low-order harmonics of the initial polarization will progressively dominate the contributions of the higher harmonics. Consequently, we may expect to obtain reasonable approximations for the functional integrals (4.4) by representing the initial polarizations by Fourier series truncated at a quite low order $\nu_{\max}$. In order to obtain a quantitative check of this conjecture let us calculate the average intensity radiated to the right during the linear regime as a function of the order of truncation $\nu_{\max}$. We obtain, by inserting the truncated Fourier series for $R_+(x,0)=R_-(x,0)^*$ in the solution (4.1) and by performing the initial-state average according to Eq. (4.4),

$$I(t)\approx\frac{4}{N}\int_0^1 dx\int_0^1 dx'\,\Theta(t-\alpha x)\Theta(t-\alpha x')I_0(2[x(t-\alpha x)]^{1/2})I_0(2[x'(t-\alpha x')]^{1/2})\sum_{\nu=0}^{\nu_{\max}}\cos 2\pi\nu(x-x')\,. \tag{6.10}$$

We note that in the limit $\nu_{\max}\to\infty$ this expression coincides with the exact result (4.2). We have plotted in Fig. 2 the result (6.10) for $\nu_{\max}=0,1,2$, and 3 as well as the exact result (4.2) for the case $\alpha=0.3$, $N=4\times10^9$. For that case the linear regime lasts roughly until $t\approx20$ and by that time the lowest-order approximation ($\nu_{\max}=0$) has accumulated a negative deviation from the exact intensity of about 25%. For increasing $\nu_{\max}$, however, we see that the exact result is quickly approached. For $\nu_{\max}=1$ the deviation has already decreased to roughly 10%.

VII. MEAN INTENSITY AND ITS VARIANCE

In order to solve the Maxwell-Bloch equations as nonlinear classical partial differential equations we have to resort to numerical means. Moreover, in view of the expression (4.4) we must construct a sufficiently large number of appropriate classical solutions to enable us to obtain reasonable approximations for the functional integrals representing the mean intensity and its higher-order moments.

For such an ensemble of solutions to be representative the initial polarizations from which they arise must adequately represent the Gaussian distribution (4.5). We have used two independent methods to specify the initial polarizations. In the first we represent $R_\pm(x,0)$ and $L_\pm(x,0)$ by truncated Fourier series and in the second by random complex numbers at a succession of points x along the cylinder. These two methods complement each other in various ways. The Fourier series method is particularly well suited, for example, to a thorough investigation of the influence of that part of function space which allows only very long wavelengths in the initial polarization. The random-number method provides an especially convenient tool for exploring the influence of shorter wavelengths. On the basis of the discussion in Sec. VI we expect the two approaches to lead to essentially the same results for the average radiated intensity and its higher-order moments. That expectation will indeed be verified in the following nonlinear analysis.

In our random-number method we have used a

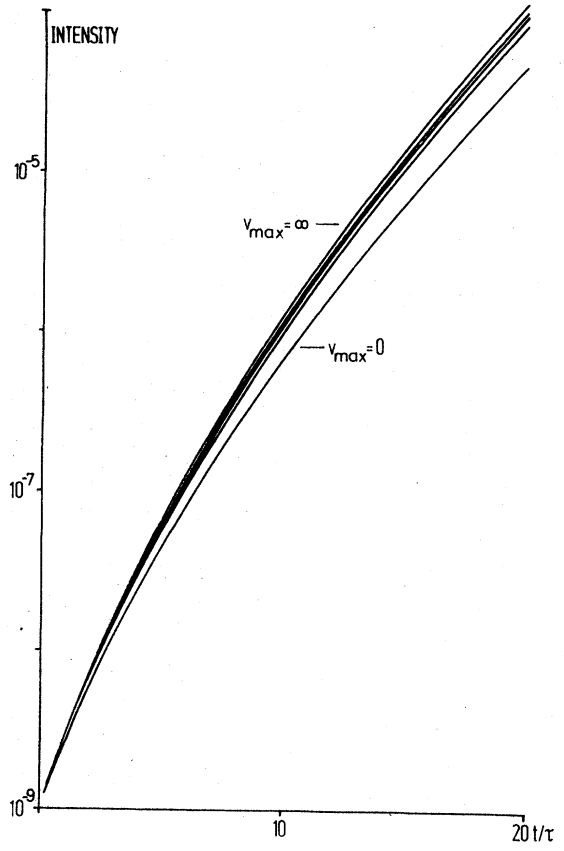

FIG. 2. Early-stage radiated mean intensity for $\alpha = 0.3$, $N = 4\times 10^9$ according to the linearized theory; the top curve corresponds to Eq. (4.2), lower ones to Eq. (6.10) with $\nu_{max} = 0$, 1, 2. and 3.

Gaussian random-number generator to assign independent values to the real and imaginary parts of $R_+(x;0)$ and $L_+(x,0)$ at a succession of 11 equally spaced points with a spacing $\Delta x = 1/10$. According to Eq. (3.3) we have chosen the Gaussian distributions to have the width $(4/N\Delta x)^{1/2}$. The functional integral (4.4) is then approximated by

$$I^n(t) = \sum |E_R^+(x=1,t,[R_+(x),L_+(x)])|^{2n}, \qquad (7.1)$$

where the sum includes all initial polarization configurations generated. The Gaussian weight present in Eq. (4.4) does not appear explicitly here. It is instead implicit in the generation of the initial polarization configurations.

If we represent the initial polarizations by the Fourier series

$$R_-(x) = R_+(x)^* = (2/\sqrt{N}) \sum_{\nu=0,\pm1,\ldots} r_\nu e^{i2\pi\nu x} \qquad (7.2)$$

and a similar series for $L_-(x) = L_+(x)^*$ with coefficients l_ν we may denote the envelope operators for the electric field by

$$E^+_{R,L}(x,t(r_\nu,l_\nu)) = E^-_{R,L}(x,t(r_\nu,l_\nu))^* . \qquad (7.3)$$

We may then express the functional integral (4.4) as a multiple integral over the Fourier coefficients r_ν and l_ν,

$$I^n(t) = \prod_{\nu=0,\pm1,\ldots} \int \frac{d^2 r_\nu}{\pi} \int \frac{d^2 l_\nu}{\pi} \exp[-(|r_\nu|^2 + |l_\nu|^2)] \times |E_R^-(x=1,t,(r_\nu,l_\nu))|^{2n} . \qquad (7.4)$$

In view of the arguments given in Sec. VI we expect, for $\alpha < 1$, only a few low-order Fourier components to contribute significantly to the functional integral (7.4). We can approximate the functional integral by truncating the infinite sequence of integrations at some modest value of $\nu = \pm\nu_{max}$.

In order to evaluate the functional integral (7.4) on the basis of a finite number of classical trajectories we not only have to truncate the Fourier series (7.2) at a finite order but also to discretize the integrals over each Fourier coefficient. We have chosen to do the integral over each complex Fourier coefficient as a double integral over its real and imaginary parts and to approximate each such real integral by the three-point version of the technique of Hermite integration.[8] For an arbitrary function $f(x)$ this approximation amounts to writing

$$\frac{1}{\sqrt{\pi}} \int_{-\infty}^{+\infty} dx\, e^{-x^2} f(x) \approx w(0) f(0) + w(|x_1|)[f(x_1) + f(-x_1)] , \qquad (7.5)$$

with certain fixed values for the weight factors w and the abscissa x_1.[8]

If we write the Fourier coefficients as

$$r_\nu = r'_\nu + i r''_\nu , \quad l_\nu = l'_\nu + i l''_\nu , \qquad (7.6)$$

the Hermite approximation (7.5) leads to the following expression for the nth intensity moment (7.4)

$$I^n(t) = \sum_{(r'_\mu + i r''_\mu,\, l'_\mu + i l''_\mu)} \left[\prod_\nu w(r'_\nu) w(r''_\nu) w(l'_\nu) w(l''_\nu)\right] |E_R^-[x=1,t,(r'_\nu + i r''_\nu, l'_\nu + i l''_\nu)]|^{2n} . \qquad (7.7)$$

In our computations for the nonlinear regime we have taken into explicit account only the six complex Fourier coefficients $r_{0,\pm1}$ and $l_{0,\pm1}$. Since we permit both the real and imaginary parts of each of them to take on three different values, the sum in Eq. (7.7) then contains 3^{12} terms. Each of these specifies a different initial condition and requires, in principle, a separate solution for E_R^- from the Maxwell-Bloch equations. Fortunately, since we have the symmetries

$$E_R^-[x,t,(r_\nu,l_\nu)]=E_L^-[1-x,t,(l_\nu,r_\nu)]\,,$$
$$E_{R,L}^-[x,t,(r_\nu^*,l_\nu^*)]=E_{R,L}^-[x,t,(r_\nu,l_\nu)]^*\,, \qquad (7.8)$$

and since the intensity

$$|E_{R,L}^-[x,t,(e^{i\phi}r_\nu,e^{i\phi}l_\nu)]|^2$$

does not depend on the phase angle ϕ we can break these 3^{12} trajectories into a much smaller number of groups each of which comprise different electric field trajectories making equal contributions to the mean value $I^n(t)$. The weight of each group in the sum (7.7) is determined by the product of the number of trajectories it contains with the factor

$$\Pi_\nu w(r_\nu')w(r_\nu'')w(l_\nu')w(l_\nu'')$$

which is, of course, the same for each member of a group. We may order these groups of trajectories according to their weight in the expectation that only the ones of greatest weight contribute significantly to the sum (7.7). This approach, as we shall see, is indeed practicable and leads to a dramatic reduction of the number of trajectories that must be calculated.

In order to integrate the Maxwell-Bloch equations for a given initial polarization we have used a numerical algorithm based on the method of characteristics. It was designed to incorporate the conservation law (5.1). We have rendered the coordinate x discrete by allowing for $M+1$ points with a spacing $\Delta x=1/M$. Correspondingly, the time t was discretized with spacing $\Delta t=\alpha\Delta x$. Since the computation time for each trajectory grows quadratically with M it is not practicable to let M be too large. Most of our calculations have been carried out with $M=10$ but several checks have been performed with $M=40$. We have compared the intensity for a typical trajectory numerically calculated using $M=10$ with the analytic result (4.1) derived for the early stages of the process. The discrepancy grows with time but never exceeds a few percent during the linear regime. In Fig. 3 we have plotted the intensity for a typical trajectory as calculated numerically with $M=10$ and $M=40$. The agreement clearly is quite satisfactory. Figure 3 also shows that the conservation law (5.2) is obeyed to within ~1% for times up to that

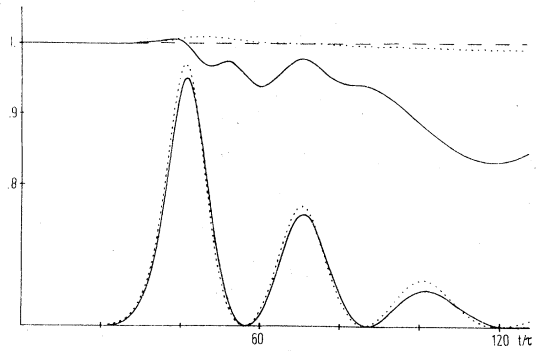

FIG. 3. Typical single intensity trajectory obtained numerically with $\Delta x=1/10$ (full curve) and $\Delta x=1/40$ (dotted curve); the upper curves show the corresponding total energies according to the left-hand side of Eq. (5.2); again, $\alpha=0.3$, $N=4\times10^9$.

of the first intensity maximum and to within 10% until the time of the third maximum. For $M=40$ the error remains of the order of 1% even beyond the third maximum.

We turn now to the calculation of the mean intensity and its variance on the basis of the Fourier series representation of the initial polarizations. For the case $\alpha=0.3$, $N=4\times10^9$ we find that it is indeed possible, as suggested earlier, to approximate the sum (7.7) by including only the rather restricted groups of trajectories bearing the greatest weight. To illustrate this technique it is instructive to carry out the sum by including in successive steps of approximation more and more groups of trajectories in order of decreasing weight. We have plotted in Fig. 4 the height $I_{\max}$ of the first maximum of the mean intensity and the time $t_{\max}$ of its occurrence as functions of the number of groups of trajectories summed over. The maximum number of groups in these calculations was 705 which together comprise 33 456 individual trajectories. It is evident from Fig. 4 that

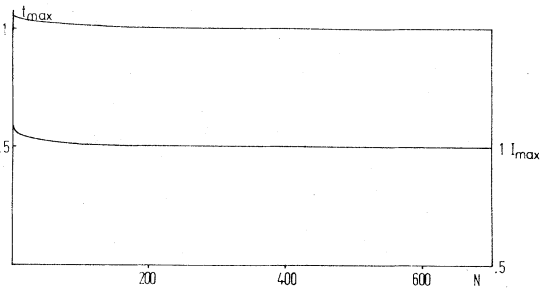

FIG. 4. Height and time of first maximum of mean intensity for partial functional integrals with N most important groups of trajectories $0<N\leq705$; both quantities are normalized to their values at $N=705$; again, $\alpha=0.3$, $N=4\times10^9$.

the convergence of the mean values is quite rapid. In fact, once the first 20 groups are included the quantities I_{max} and t_{max} are changed by less than 5% by adding the remaining 685 groups.

The results for the mean intensity and its variance calculated by using all 705 groups are displayed in Fig. 5. The mean intensity shows a high first peak and subsequent ringing. The intensity minima are not zeros. The variance has an interesting structure with maxima at times near those at which the mean intensity changes most rapidly and with minima near times at which the intensity is stationary. This structure suggests that a significant part of the variance may be due to a fluctuating delay time for the appearance of pulses having the general form of the mean intensity curve. On the other hand, the fact that the minima of the variance are not very small shows clearly that other kinds of fluctuations such as variations of the strengths of the maxima are also present. A selection of calculated pulses which illustrates the fluctuations present is shown in Fig. 6. We shall discuss these fluctuations in more detail in Sec. VIII.

As a further check we have evaluated the mean radiated intensity and its variance by using the random-number realization of the initial polarization values. The calculation was based on a representative sample of 150 trajectories each of which was integrated on a spatial grid with $M = 10$. The resulting curves are identical in structure to those of Fig. 5. The only noteworthy difference is a small decrease of the delay time t_{max}. The smallness of this difference is a satisfactory confirmation of the dominance of long-wavelength fluctuations discussed earlier. The fact that a small decrease rather than an increase is obtained can be understood on the basis of Fig. 2. Adding the effects of higher harmonics in the initial polarization makes the intensity rise a little more rapidly.

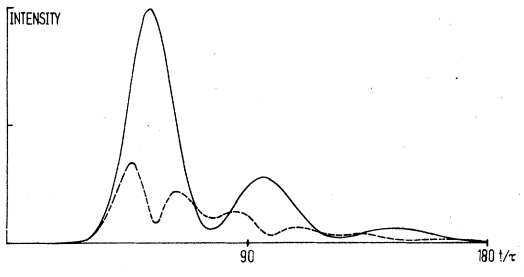

FIG. 5. Mean intensity and its variance (dashed) obtained numerically according to Eq. (7.7) from the 705 most important groups of trajectories for $\alpha = 0.3$, $N = 4 \times 10^9$.

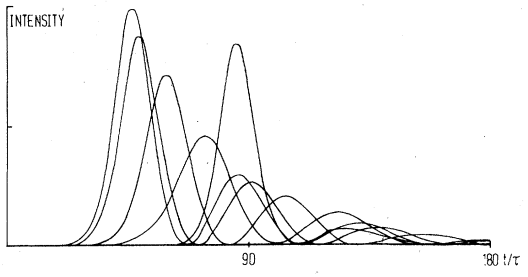

FIG. 6. Typical single intensity trajectories for $\alpha = 0.3$, $N = 4 \times 10^9$.

VIII. PULSE STATISTICS

According to the arguments given in Sec. V the ensemble of classical trajectories generated by a Gaussian distribution of initial polarizations constitutes an ensemble of experimentally observable pulses. We can therefore draw much more information from the set of trajectories calculated numerically than just the mean intensity and its variance. As examples which may be experimentally measurable we display the histograms for the distributions of the first intensity maximum $I_{max} = |E_R^-(1,t)|^2_{max}$ and for the delay time t_{max} at which the maximum occurs in Figs. 7 and 8, respectively. These histograms are based on 150 trajectories which arise from the random-number realization of the initial polarizations. We can infer from these histograms that I_{max} and t_{max} have variances which are as large as 18% and 12% of the respective mean values. Other parameters which characterize the pulse shape such as the duration of the first intensity peak and the ratio of the first and second intensity maxima in each trajectory undergo similarly large fluctuations.

We have noted earlier that the atomic system emits two pulses, one traveling in each direction along the cylinder axis. It is interesting to compare the statistical properties of these two pulses.

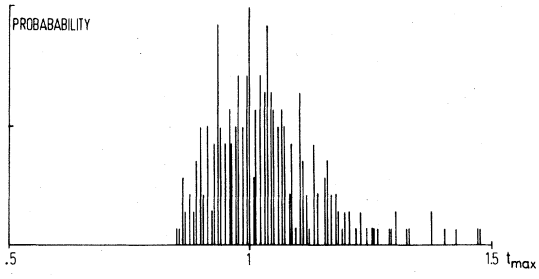

FIG. 7. Distribution of delay times of first intensity maxima within an ensemble of 150 trajectories calculated by using the random-number realization of the initial polarization; the time is normalized to the delay time of the mean intensity; again, $\alpha = 0.3$, $N = 4 \times 10^9$.

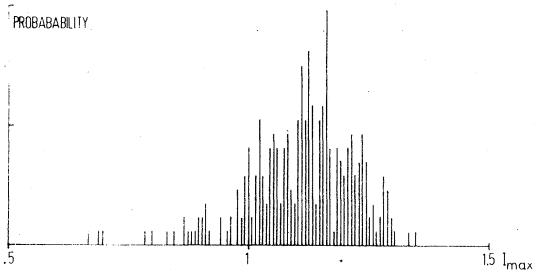

FIG. 8. Distribution of heights of first intensity maxima within an ensemble of 150 trajectories calculated by using the random-number realization of the initial polarization; the height is normalized to the height of the mean intensity; again, $\alpha = 0.3$, $N = 4 \times 10^9$.

As a quantity which should be especially easy to observe experimentally we have considered the difference of the first intensity maxima of the right- and left-going pulses. A histogram of the distribution of these differences for 150 trajectories is shown in Fig. 9. The clustering of these differences about the value zero indicates a tendency for the pulses to be radiated symmetrically.

IX. CONCLUSIONS

Although there have been a number of observations of superfluorescent pulses there are not yet sufficient experimental data to compare with the full content of our results.

The conditions of applicability of the present theory in which we have omitted all radiationless decay mechanisms are probably best met in some of the experiments of Gibbs, Vrehen, and Hikspoors[2(e),2(f)] based on beams of Cs atoms. There the incoherent decay times T_1 and T_2 of the atomic inversion and polarization, respectively, and the dephasing time T_2^* of the polarization are sufficiently large compared to the observed pulse widths and delays to render the effects of incoherent and inhomogeneous broadening negligible. Moreover, these experiments were done for Fresnel numbers close to unity so that our assumption (2.14) of two weakly modulated plane waves traveling in opposite directions should not be unreasonable.

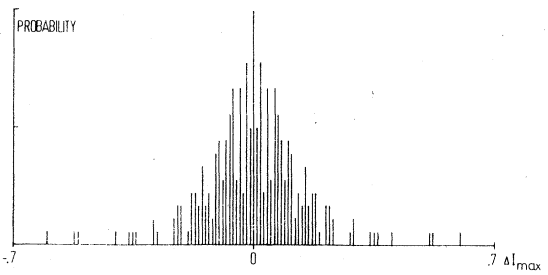

FIG. 9. Distribution of the intensity difference ΔI_{max} of the first peaks of the pulses radiated to the left and the right; again, $\alpha = 0.3$, $N = 4 \times 10^9$.

However, the fluctuations of the radiated intensity from one experimental pulse to another seem thus far to be due as much to uncontrollable conditions in the experiments as to the intrinsic quantum noise discussed in the present paper.[9] For example, neither the number density of initially excited atoms nor the precise shape and size of the active volume are under sufficient control to permit the measurement of an ensemble of pulses for given values of the parameters α and N. There are thus no published experimental data as yet on the statistics of superfluorescent pulses or even the mean radiated intensities. A preliminary inspection of the existing data suggests, however, that they may not be incompatible with the statistics we predict for the pulse delay times t_{max}.[9,2(h)]

The four pulse shapes published in Ref. 2(f) are individual examples rather than mean values. In order to check on the compatibility of the respective delay times with our results we have indicated the observed delay times for the four corresponding values of the number density of atoms, n, in Fig. 10. The horizontal bars through the experimental delay times describe the uncertainty of n given in Ref. 2(f). The curves in Fig. 10 present the density dependence of the numerically calcu-

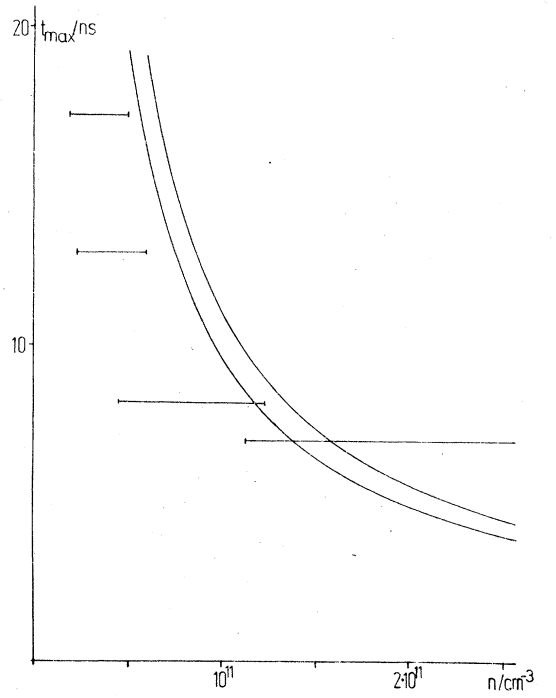

FIG. 10. Delay time of first maximum of the mean intensity as a function of the number density of atoms for the parameters corresponding to the 2-cm-beam experiment of Ref. 2(f).

lated delay time of the first peak of the average intensity. These curves were obtained by using the values for λ, τ_0, and l given in Ref. 2(f). The upper curve which implies slightly larger delay times is based on the Fourier series realization of the initial polarization and the lower one on the random-number realization. The agreement, as we see, is provisionally satisfactory.

While our present results clearly call for new experimental data on the statistics of superfluorescent pulses, it is only fair to say that the existing data seem to present theory with difficulties, too. For instance, if we assume the four experimental pulses mentioned to be typical of their respective (α, N) ensembles we are facing durations of the first intensity peak larger by perhaps as much as a factor of 2 than typical durations occurring in the theoretical ensembles. Moreover, the experimental pulses show distinctly less structure in their tails than the theoretical ones, i.e., they don't give any clear indication of the ringing which is evident in the pulses of Fig. 6. These discrepancies are an interesting subject for speculation. It seems unlikely to us that inhomogeneous broadening play a significant role, since for the beam experiments of Ref. 2(f) one has $t_{max}/T_2^* < 0.5$. Nor should the competition of the axial modes considered here with the neighboring off-axial modes be an important effect for a system with a Fresnel number of order unity.

It is quite conceivable, however, that the difficulty lies in the relation of the one-dimensional problem we have defined to the actual problem in three dimensions. We have noted in Sec. II that for Fresnel number 1 the radial dependence of the fields is not truly negligible. Furthermore, because of the way in which the atoms are excited, the density within the cylinder is not uniform but a decreasing function of radius. For that reason alone the fields within the cylinder will decrease rapidly as functions of the radius. If the cylinder had a Fresnel number large compared to 1 it would be possible to treat its axial modes by ray optics, that is, by regarding the cylinder in effect as a bundle of parallel uniform fibers and treating the wave propagation down each of the fibers independently. For Fresnel number 1 this approximation is only marginally applicable but it should nonetheless indicate the kind of correction to be anticipated from a three-dimensional treatment.

According to this picture the total radiated field is the sum of the fields contributed by the end faces of all of the fibers. The fibers which are further from the axis will have smaller densities of excited atoms and lower amplification rates. The pulses they radiate will thus have larger delay times. If this picture is correct the fibers closest to the axis should furnish the fields which amplify most rapidly. These contributions should dominate the early parts of the radiated pulse and play the most important role in determining the delay time. The pulses from the outer fibers would then appear later and be responsible for lengthening the first intensity peak and washing out the subsequent ringing. The radiation pattern according to this picture would presumably change rapidly in time.

Finally this picture suggests that the delay times calculated in this paper may be in better agreement with the experimental values of Ref. 2(f) than is indicated in Fig. 10. If the delay times are indeed determined predominantly by the central density of the excited atoms rather than by the average density, the experimental points in Fig. 10 could be moved significantly toward higher densities.

Let us recall the main results of the present investigation and cast them into the perspective of prior work. While each superfluorescent pulse may, except for its very early stage, be looked upon as a classical process, the ensemble of such pulses starting from physically identical initial states displays large fluctuations. All quantities characterizing the shape of the pulses vary strongly enough within the ensemble that their variances assume the same orders of magnitude as their mean values. The feature of superfluorescence just described is common to all macroscopic processes where an unstable equilibrium state decays due to the action of microscopic fluctuations. As the decay takes place fluctuations which are initially tiny grow to macroscopic size since they are not inhibited by restoring forces at the instability. When a stable equilibrium state is eventually approached large restoring forces become operative and subdue the fluctuations to a normal level again, unless the final state corresponds to a critical point. Other examples of such processes are the switch-on of a laser,[5,10] the buildup of order in a magnet after quenching below the Curie temperature, and the reversal of order in a ferromagnet after the reversal of an external magnetic field.[11]

Most previous studies of the statistical properties of superfluorescence have been done in the framework of the single-mode model [Refs. 3(b), 3(c), 3(e)–3(h), 3(m), 3(n), 3(p), and 3(q)]. In proposing this model Bonifacio, Schwendimann, and Haake[3(f)] argued that for systems with a length $l \ll l_c$ the photon escape time l/c is small compared to the superfluorescence time. In that case the electric field within the active volume will tend to follow the behavior of the atoms with no inertial lag. The single-mode model implements this idea by simply replacing the Maxwell equa-

tion for the electric field by the adiabatic correspondence $\hat{R}_{\pm} = \hat{E}_R^{(\mp)}$. Bonifacio and Lugiato in later work[3(p)] have generalized this adiabatic correspondence to include an inertia term, $\alpha\dot{\hat{E}}^{\mp} + \hat{E}^{\mp} = \hat{R}_{\pm}$.

The single-mode model clearly oversimplifies the pulse dynamics by disregarding entirely the propagation of the electric field in space. However, it has the great virtue of admitting an analytic treatment of its statistical behavior[3(f)-3(h),3(q)] and yields qualitative insight into many aspects of the decay of the initial state. Moreover, it even seems to account for some experimental data in at least a semiquantitative manner.[12] Finally, the explicit solution for the statistical behavior of the single-mode model has provided us the strategy we have used in the present investigation which includes the missing propagation effects.[3(h)]

There is one feature, however, of the single-mode model which cannot be reconciled with the results of the present study. The model predicts that all pulses emerging from a given system have identical hyperbolic secant shapes and differ only in the delay times. The delay times can then be expressed in terms of a small effective initial tipping angle θ_0 which is defined as the ratio of the initial atomic polarization to the initial atomic inversion. We find, however, that the ensemble of pulses we have calculated cannot be represented by any such one-parameter family of curves.

Since the "initial tipping angle" has become a rather widely used concept for treating spontaneous emission in classical terms we would like to emphasize that the initial condition for a single pulse cannot be characterized by a single number like an angle. Instead, the polarization configurations $R_{\pm}(x,t=0)$ and $L_{\pm}(x,t=0)$ must be used. It is only the average behavior of an ensemble of identical systems that can be characterized by an effective tipping angle. To do that we may write Eq. (3.4) in the form

$$\langle\{\uparrow\}|R_+(x)R_-(x')|\{\uparrow\}\rangle = \sin^2\theta_0\,\delta(x-x')$$

with the initial noise strength

$$\sin\theta_0 \approx \theta_0 = 2/\sqrt{N}\,. \tag{9.1}$$

Vrehen and Schuurmans[2(h)] have recently reported an experiment on vapor of cesium atoms which confirms the initial noise strength to be of order $1/\sqrt{N}$.

Several workers have treated superfluorescence by replacing the quantum-mechanical Maxwell-Bloch equations by c-number equations and numerically calculating classical trajectories for the radiated field.[3(r),3(s),12] Our present treatment differs from these by including correctly the influence of quantum fluctuations on the ensemble of radiated pulses. We have also presented arguments to show that corrections to the classical dynamics are only of the order $1/\sqrt{N}$ after the initial stages of the process.

Ressayre and Tallet have calculated the mean radiated intensity in the limit of small α by decoupling the hierachy of equations of motion for expectation values which follow from the quantum-mechanical Maxwell-Bloch equations.[3(u)] Their results seem to be in reasonable agreement with ours.

In a recent paper Polder, Schuurmans, and Vrehen[3(w)] discuss the initial linear part of the amplification process. They too have derived a quantum-mechanical formulation of superfluorescent pulses in terms of stochastic c-number fields. Since they have chosen a formal framework especially well suited for calculating expectation values of antinormally ordered products of field operators they were led to initial values of the polarization that vanish for all trajectories. The fluctuations initiating the decay of the initial state show up as random forces in the equation of motion for the polarization. The equivalence of their results to ours for the linear stages of the process can most easily be inferred from an argument recently given by one of us.[5]

Hopf[18] has recently suggested that our truncation of the Fourier series (7.2) for the initial polarizations at low orders and the gridding of the space coordinate by 11 points suppresses certain dynamical disturbances of the relative phase between the polarization and the electric field which might modify the pulse statistics. While this suggestion has the arguments of Sec. VI against it, it has some support in Hopf's treatment of the swept-gain amplifier.[13] We are therefore investigating it further.

ACKNOWLEDGMENTS

We would like to thank D. Polder, M. F. H. Schuurmans, Q. H. F. Vrehen, and F. Hopf for most fruitful discussions. We are also grateful to F. Hopf for help in finding a numerical error. We have enjoyed an enlightening correspondence with R. Bonifacio. We gratefully acknowledge financial support by a NATO Research Grant No. 1445 and by the U. S. Department of Energy under Contract No. EY 76-02-3064. We have appreciated the generous amount of computation time allotted to us by the Rechenzentrum der Universität Düsseldorf und der Gesamthochschule Essen.

APPENDIX

The result (4.4) which expresses the quantum-mechanical expectation values of normally or-

dered products of field operators as averages over classical trajectories can also be derived in the following way.

The Maxwell-Bloch equations (2.17) for the envelope operators may be looked upon as the Heisenberg equations of motion for the effective Hamiltonian:

$$\frac{1}{\hbar}H=-i\frac{N}{4}\int dx\left(\hat{E}_R^-(x)\frac{\partial}{\partial x}\hat{E}_R^+(x)-\hat{E}_L^-(x)\frac{\partial}{\partial x}\hat{E}_L^+(x)\right)$$
$$+i\frac{N}{4}\int dx\left(\hat{E}_R^-(x)\hat{R}_-(x)+\hat{E}_L^-(x)\hat{L}_-(x)-\text{H.c.}\right). \tag{A1}$$

In order to demonstrate this one has to use the commutation relations of the envelope operators. The relevant commutators read

$$[\hat{R}_+(x),\hat{R}_-(x')]=[\hat{L}_+(x),\hat{L}_-(x')]$$
$$=\frac{4}{N}\delta(x-x')\hat{Z}(x'),$$
$$[\hat{Z}(x),\hat{R}_\pm(x')]=\pm\frac{2}{N}\delta(x-x')\hat{R}_\pm(x), \tag{A2}$$
$$[\hat{Z}(x),\hat{L}_\pm(x')]=\pm(2/N)\delta(x-x')\hat{L}_\pm(x),$$
$$[\hat{E}_R^+(x),\hat{E}_R^-(x')]=[\hat{E}_L^+(x),\hat{E}_L^-(x')]=\frac{4}{\alpha N}\delta(x-x').$$

The commutators (A2) follow from the definitions (2.13) and (3.1) of the smoothed envelope operators. We note that the commutators are all of order $1/N$.

Let the density operator $\rho(t)$ of the system be represented by the moment-generating functional

$$\text{tr}\,\mathfrak{O}([r_\pm(x),l_\pm(x),z(x),e_{R,L}^\pm(x)])\rho(t)$$

with

$$\mathfrak{O}=\left[\exp i\int dx\,(r_+\hat{R}_++l_+\hat{L}_+)\right]\left(\exp i\int dx\,z\hat{Z}\right)\left[\exp i\int dx\,(r_-\hat{R}_-+l_-\hat{L}_-)\right]$$
$$\times\left[\exp i\int dx\,(e_R^-\hat{E}_R^-+e_L^-\hat{E}_L^-)\right]\left[\exp i\int dx\,(e_R^+\hat{E}_R^++e_L^+\hat{E}_L^+)\right]. \tag{A3}$$

Obviously, by evaluating functional derivatives of this generating functional with respect to the auxiliary fields $r_+(x)=r_-(x)^*$, $z(x)=z^*(x)$, etc., for vanishing values of these fields we can generate expectation values of normally ordered operators such as

$$\langle\hat{R}_+\hat{L}_+\hat{Z}\hat{R}_-\hat{L}_-\hat{E}_R^-\hat{E}_L^-\hat{E}_R^+\hat{E}_L^+\rangle. \tag{A4}$$

It is slightly more convenient to work with the functional Fourier transform of the generating functional,[14-17]

$$P((R_\pm,L_\pm,Z,E_{R,L}^\pm),t)=\int d^2r_+\,d^2l_+\,dz\,d^2e_R^-\,d^2e_L^-\exp-i\int dx\,(r_+R_++r_-R_-+zZ+l_+L_++l_-L_-+e_R^-E_R^-+e_R^+E_R^+$$
$$+e_L^-E_L^-+e_L^+E_L^+)\,\text{tr}\,\mathfrak{O}\rho(t). \tag{A5}$$

This Fourier transform is a quasiprobability distribution. It has a c-number field $X(x)$ associated with each envelope operator $\hat{X}(x)$ such that the normally ordered expectation values (A4) are moments of P with respect to the corresponding c-number fields.

The Liouville–von Neumann equation for the density operator,

$$\dot{\rho}(t)=-(i/\hbar)[H,\rho(t)], \tag{A6}$$

implies an equation of motion for the quasiprobability P. This equation is easily found by using the commutation relations (A2) and the ensuing identities

$$E_{R,L}^-(x)\mathfrak{O}=\frac{\delta}{\delta ie_{R,L}^-(x)}\mathfrak{O},$$
$$E_{R,L}^+(x)\mathfrak{O}=\left\{\frac{4}{\alpha N}ie_{R,L}^-(x)+\frac{\delta}{\delta ie_{R,L}^+(x)}\right\}\mathfrak{O},$$
$$R_+(x)\mathfrak{O}=\frac{\delta}{\delta ir_+(x)}\mathfrak{O}, \tag{A7}$$
$$R_-(x)\mathfrak{O}=\left\{\left(-\frac{2}{N}ir_+(x)\right)^2\frac{\delta}{\delta ir_+(x)}-\frac{4}{N}ir_+(x)\frac{\delta}{\delta iz(x)}\right.$$
$$\left.+\left(\exp\frac{2}{N}iz(x)\right)\frac{\delta}{\delta ir_-(x)}\right\}\mathfrak{O}.$$

It reads

$$\dot{P}=LP, \tag{A8}$$

with

$$L=-\int dx\left\{\frac{\delta}{\delta R_+(x)}Z(x)E_R^-(x)-\frac{1}{2}\frac{\delta}{\delta Z(x)}E_R^-(x)R_-(x)+\frac{1}{\alpha}\frac{\delta}{\delta E_R^-(x)}\left(R_+(x)+\frac{\partial E_R^-(x)}{\partial x}\right)-\frac{1}{N}\frac{\delta^2}{\delta R_+(x)^2}R_+(x)E_R^-(x)\right.$$
$$\left.+\frac{N}{4}\left[\exp\left(-\frac{2}{N}\frac{\delta}{\delta Z(x)}\right)+\frac{2}{N}\frac{\delta}{\delta Z(x)}-1\right]R_-(x)E_R^-(x)+\text{c.c.}+\text{same with right}\rightleftharpoons\text{left}\right\}. \quad \text{(A9)}$$

We see that functional derivatives of order n occurring in Eq. (A9) have an explicit factor $(1/N)^{n-1}$. This is, of course, a consequence of the factors $1/N$ in the commutators (A2). If all terms with factors $1/N$ are neglected in L, Eq. (A8) becomes a first-order functional differential equation which can be solved by the method of characteristics. The corresponding characteristic equations are just the classical Maxwell-Bloch equations (2.17).

The second- and higher-order derivatives in L can indeed be dropped in the limit of large N. The error thus made does not affect the physically interesting low-order moments of P by more than corrections of order $1/N$. This is quite easily seen by extracting from Eq. (A8) equations of motion for such moments.

Since we have defined the quasiprobability so that it has normally ordered expectation values like (A4) as its moments it takes the form (3.7) initially. The result (4.4) for the moments of the radiated intensity then follows from

$$I^n(t)=\int d^2E_R^-\,d^2E_L^-\,d^2R_-\,d^2L_-\,dZ\,|E_R^-|^{2n}P(t)\,. \quad \text{(A10)}$$

We can derive it by inserting the solution $P(t)$ reached by the method of characteristics and using the initial fields as integration variables.

[1] R. M. Dicke, Phys. Rev. 93, 493 (1954).

[2] (a) N. Skribanowitz, J. P. Herman, J. C. MacGillivray, and M. S. Feld, Phys. Rev. Lett. 30, 309 (1973); (b) M. Gross, C. Fabre, P. Pillet, and S. Haroche, *ibid.* 36, 1035 (1976); (c) A. Flusberg, T. Mossberg, and S. R. Hartmann, Phys. Rev. Lett. A 58, 373 (1976); (d) A. T. Rosenberger, S. J. Petuchowsky, and T. A. Temple, in *Cooperative Effects in Matter and Radiation*, edited by C. M. Bowden, D. W. Howgate, and H. R. Robl (Plenum, New York, 1977); (e) Q. H. F. Vrehen, H. M. J. Hikspoors, and H. M. Gibbs, Phys. Rev. Lett. 38, 764 (1977); (f) H. M. Gibbs, Q. H. F. Vrehen, and H. M. J. Hikspoors, *ibid.* 39, 547 (1977); (g) P. Duhm and J. Marek (unpublished); (h) Q. H. F. Vrehen and M. F. H. Schuurmans, Phys. Rev. Lett. 42, 224 (1979).

[3] (a) V. Ernst and P. Stehle, Phys. Rev. 176, 1456 (1968); (b) R. H. Lehmberg, *ibid.* 181, 32 (1969); Phys. Rev. A 2, 833 (1970); (c) G. S. Agarwal, Phys. Rev. 178, 2025 (1969); Phys. Rev. A 2, 1730 (1970); (d) D. Dialetis, *ibid.* 2, 599 (1970); (e) N. W. Rehler and J. H. Eberly, *ibid.* 3, 1735 (1971); (f) R. Bonifacio, P. Schwendimann, and F. Haake, *ibid.* 4, 302 (1971); *ibid.* 4, 854 (1971); (g) V. Degiorgio, Opt. Commun. 2, 362 (1971); (h) F. Haake and R. Glauber, Phys. Rev. A 5, 1457 (1972); (i) R. Friedberg and S. R. Hartmann, Phys. Lett. A 38, 227 (1972); Opt. Commun. 10, 298 (1974); Phys. Rev. A 10, 1728 (1974); (j) R. Friedberg, S. R. Hartmann, and J. T. Manassah, Phys. Lett. A 40, 365 (1972); (k) G. Oliver and A. Tallet, Phys. Rev. 7, 1061 (1973); (l) E. Ressayre and A. Tallet, Phys. Rev. Lett. 30, 1239 (1973); (m) G. Banfi and R. Bonifacio, *ibid.* 33, 1259 (1974); Phys. Rev. A 12, 2068 (1975); (n) L. M. Narducci, C. A. Coulter, and C. M. Bowden, *ibid.* 9, 829 (1974); (o) E. Ressayre and A. Tallet, *ibid.* 11, 981 (1975); *ibid.* 12, 1725 (1975); *ibid.* 15, 2410 (1977); (p) R. Bonifacio and L. A. Lugiato, *ibid.* 11, 1507 (1975); *ibid.* 12, 587 (1975); (q) R. Glauber and F. Haake, *ibid.* 13, 357 (1976); (r) J. C. MacGillivray and M. S. Feld, *ibid.* 14, 1169 (1976); (s) R. Saunders, S. S. Hassan, and R. K. Bullough, J. Phys. A 9, 1725 (1976); (t) E. Ressayre and A. Tallet, Phys. Rev. Lett. 37, 424 (1976); (u) E. Ressayre and A. Tallet, Phys. Rev. A 18, 2196 (1978); (v) R. Glauber and F. Haake, Phys. Lett. 68A, 29 (1978); (w) D. Polder, M. F. H. Schuurmans, and Q. H. F. Vrehen, J. Opt. Soc. Am. 68, 699 (1978); Phys. Rev. A 19, 1192 (1979).

[4] *Cooperative Effects in Matter and Radiation*, edited by C. M. Bowden, D. W. Howgate, and H. R. Robl (Plenum, New York, 1977).

[5] F. Haake, Phys. Rev. Lett. 41, 1685 (1978).

[6] W. Heitler, *The Quantum Theory of Radiation*, (Oxford University, New York, 1954).

[7] F. T. Arecchi and E. Courtens, Phys. Rev. A 2, 1730 (1970).

[8] *Handbook of Mathematical Functions*, edited by M. Abramovitz and I. A. Stegun (Dover, New York, 1970).

[9] Q. H. F. Vrehen (private communication).

[10] F. T. Arecchi and V. Degiorgio, Phys. Rev. A 3, 1108 (1971).

[11] K. Kawasaki, M. C. Yalabik, and J. D. Gunton, Phys. Rev. A 17, 455 (1978) (and references given therein).

[12] R. Bonifacio *et al.* in Ref. 4.

[13] F. A. Hopf and E. A. Overman II, Phys. Rev. A 19, 1180 (1979).

[14] This quasiprobability generalizes the one used in Ref. 3(h) to the case of position-dependent fields; correspondingly, the functional differential equations (A8) and (A9) reduces to the partial differential equation (3.4) of Ref. 3(h) by: (i) taking the fields to be spatially homogeneous; (ii) depriving the electric field of its independent dynamics by imposing the adiabatic correspondence

$E_R^{\pm} = R_{\mp}$; and (iii) neglecting the coupling between the right- and left-running waves.

[15]R. J. Glauber, Phys. Rev. 131, 2766 (1963).
[16]H. Haken, H. Risken, and W. Weidlich, Z. Phys. 206, 355 (1967).
[17]R. Graham and H. Haken, Z. Phys. 234, 193 (1970); 235, 166 (1970).
[18]F. Hopf, Phys. Rev. A 20, 2064 (1979).